e-mail: `jhniede@sandia.gov`

Magnetic-pulse-driven Rayleigh-Taylor instability in plastically deforming metals

John NIEDERHAUS[1], Scott ALEXANDER[1], Tom HAILL[1], Tracy VOGLER[1] and Jim ASAY[1]

[1] *Sandia National Laboratories, Albuquerque, NM USA*

Abstract: A series of two-dimensional finite-element simulations are carried out using the finite element multimaterial magnetohydrodynamics code ALEGRA for Rayleigh-Taylor instability of an interface between plastically deforming metals, under the unsteady acceleration associated with magnetic pressure generated by a pulsed-power device. For an aluminum-copper interface under a 10-GPa-peak driving pressure, the perturbation exhibits exponential growth for a short time, followed by a "coasting" phase characterized by growth at a constant rate. The yield strength of the copper material is varied artificially by adjusting pressure- and strain-hardening parameters in the material strength model, and consequent changes in the exponential growth rate across a range of perturbation wavelengths are found to agree with the simple fluid model of Colvin *et al.* [1] to within less than 50%. The applicability of the Colvin model for this problem is found to be questionable, however, due to the variable nature of the acceleration, and to distinctions between fluid and plastic flow. Simulation results indicate that perturbation growth is sufficiently sensitive to material yield strength for the design of experiments to infer yield strength from observed instability growth, using existing pulsed-power facilities.

1 INTRODUCTION

It is well known that the ability of a material to sustain shear loading, and its tendency to yield under stresses beyond the elastic limit, can significantly alter the details of Rayleigh-Taylor (RT) instability growth in the material. RT instability growth in plastically deforming solids has been observed and analyzed in many contexts. Here, the possiblity is investigated that a material's yield strength may be inferred from RT-induced plastic deformation observed in the material, driven by the unsteady acceleration associated with Lorenz forces generated by a pulsed-power device.

First, a preliminary discussion of RT growth in materials with strength is presented. Then, experimental schemes are outlined which have been used to measure material strength via RT growth. Third, numerical modeling for such systems using finite-element magnetohydrodynamic (MHD) simulations is discussed, and an approach suggested for experiment design within a number of constraints. Finally, results from numerical parameter studies for RT growth on an alumnium-copper interface in plastic deformation are presented, and the results interpreted in light of theoretical considerations. Conclusions are drawn on this basis as to the feasibility of an experimental measurement of material strength using RT growth.

2 RAYLEIGH-TAYLOR INSTABILITY IN MATERIALS WITH STRENGTH

Strength is the ability of a material to sustain shear stresses; it is characterized by the yield stress Y, which is the stress at which deformation of the material becomes thermodynamically and kinematically irreversible. For stresses exceeding Y, the deformation is plastic rather than elastic, and upon unloading the specimen must follow a different trajectory in stress-strain space than it followed during loading, finally reaching a higher-strain state than prior to loading.

The yield stress Y may vary strongly with certain aspects of the state of the material, including the pressure p, temperature T, strain ϵ and strain rate $\dot{\epsilon}$. Such variations become particularly important at high pressures and temperatures, and high deformations. Steinberg *et al.* (1980) [2] have produced a reliable and widely used model for the yield stress of many nonferrous metals under such conditions, which may be expressed as

$$Y_{SG} = Y_0 \left[1 + \beta(\epsilon_I + \epsilon)^n\right] \left[1 + A\frac{p}{\eta^{1/3}} - B(T - 300)\right]. \tag{2.1}$$

In this expression, the following symbols denote tabulated quantities obtained from experimental data: the ambient-pressure/temperature yield stress Y_0, the strain hardening coefficient β and exponent n, the pressure hardening coefficient A, and the temperature hardening coefficient T. The parameter η is the compression, which is computed as the ratio of specific volume to initial specific volume. The model also includes a maximum yield strength Y_{max}, beyond which the yield stress is invariant.

Material strength allows a sample to deform elastically for stresses less than Y. Since the slope of the stress-strain curve is generally higher in the elastic than in the plastic regime, this elastic phase of deformation may be thought of as slowing the deformation. This resistance associated with material strength may slow the deformation due to RT instability, or it may suppress the growth completely. For materials in plastic deformation, Colvin *et al.* (2004) speculate that material strength resists plastic defomation as an effective "lattice viscosity," with a kinematic coefficient of viscosity given by

$$\nu_{\text{eff}} = \frac{Y}{\sqrt{6}\rho|\dot{\epsilon}|}, \tag{2.2}$$

where ρ denotes the density and $|\dot{\epsilon}|$ the magnitude of the strain rate in the material. Given this effective viscous dissipation in the deforming material, Colvin *et al.* then use an analysis similar to that of Mikaelian (1996) [3] to obtain a dispersion relationship for the growth of unstable modes.

Mikaelian's analysis begins with the eigenvalue equation of Chandrasekhar (1968) [4], for the stability of superposed viscous fluids with surface tension on the interface between them (which appears as equation 41 in Chapter X). Mikaelian integrates the eigenvalue equation for superposed finite-thickness fluid layers, obtaining a dispersion relation (Equation 26 in reference [3]) which relates the instability growth rate γ to a perturbation wavenumber k, a kinematic viscosity coefficient ν, an acceleration g, an Atwood number A, and a thickness h of the superposed fluid layers. A cutoff wavenumber k_c also appears in the expression, associated with RT supression by surface tension, and is given as a function of the surface tension T.

Colvin *et al.* (2004) note an analogy between viscous and surface-tension resistance to instability growth in Mikaelian's analysis and resistance due to material strength. They adapt Mikaelian's analysis to the situation where the medium has strength Y and shear modulus G by making the substitutions $\nu \to \nu_{\text{eff}}$ and $T \to G/k$. Following Mikaelian (1996), they integrate the eigenvalue equation to obtain the following dispersion relation:

$$\gamma^2 + 2k^2\nu_{\text{eff}}\gamma + k\tanh(kh)\left(\frac{kG}{\rho} - Ag\right) = 0, \tag{2.3}$$

which is solved to yield the growth rate,

$$\gamma = \nu_{\text{eff}}k^2\left(\sqrt{1 - \frac{C}{\nu_{\text{eff}}^2 k^3}} - 1\right), \tag{2.4}$$

with the sensitivity to the layer thickness incorporated in the coefficient C, defined as

$$C = \tanh(kh)\left(\frac{kG}{\rho} - Ag\right). \tag{2.5}$$

Lorenz *et al.* (2005) [5] apply this formula to study the case of plastically deforming materials, in which the elastic limit has been exceeded and the shear modulus G is zero. In this case, we have $C = -Ag\tanh(kh)$, and the model growth rate is

$$\gamma = \nu_{\text{eff}}k^2\left(-1 + \sqrt{1 + \frac{Ag}{\nu_{\text{eff}}^2 k^3}\tanh(kh)}\right). \tag{2.6}$$

The particular case studied by Lorenz *et al.* involves a plate (h=35.6 μm) of aluminum alloy 6061 accelerated by the stagnation of a laser-ablated plasma on an epoxy layer covering the aluminum sample ($A \approx 0.39$), up to a pressure of approximately 20 GPa and a strain rate of approximately $|\dot{\epsilon}| = 1\ \mu\text{s}^{-1}$. Evaluating the Colvin formula of Equation 2.6 for these conditions, over a range of artificially modified yield stresses and perturbation wavelengths, produces the growth rate trends shown in Figure 2.1. The acceleration is estimated by $g = p/(\rho h)$, where p is the peak pressure, h is the sample thickness, and ρ is the sample material density. Here, the yield strength appearing the model is modified by a multiplier Y' to produce the curves shown, and the growth rate is plotted as a function of the perturbation wavelength $\lambda = 2\pi/k$. Similarly, the Colvin formula is evaluated

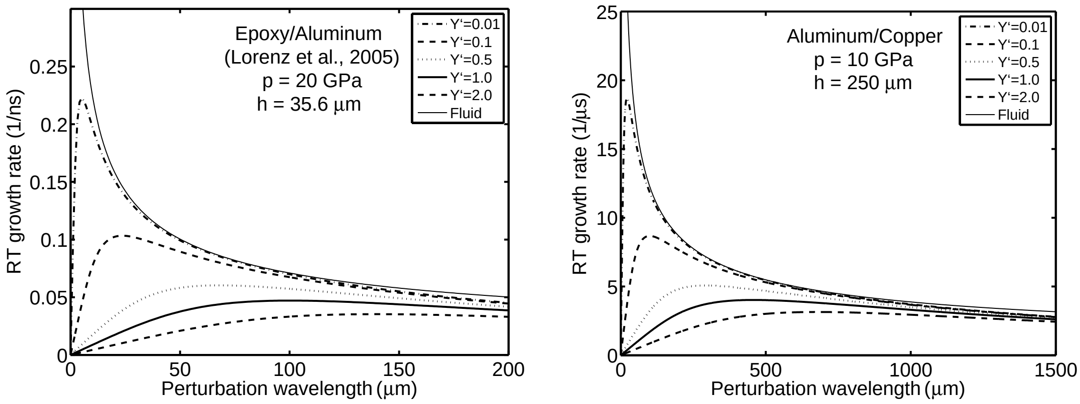

Fig. 2.1. Rayleigh-Taylor growth rates γ computed for (left) the conditions of Lorenz *et al.* (2005) [5] and (right) an aluminum-copper interface accelerated at 10 GPa, using the model of Colvin *et al.* (1998) [1], given in equation 2.6.

for a case considered below, where an aluminum-copper interface ($A \approx 0.53$) is accelerated at 10 GPa, and the yield strength of copper is modified in the same way. These predicted growth rates are also shown in Figure 2.1. (The strain rate used here is $|\dot{\epsilon}| = 0.5\ \mu s^{-1}$, and the copper plate is assumed to have a thickness h=250 μm). Note that the growth rate γ is the exponent of linear RT growth, where the perturbation amplitude grows in time as $\eta(t) \propto e^{\gamma t}$.

The variation in the RT growth exponent with yield strength multiplier Y' and the perturbation wavelength λ shown in Figure 2.1 exhibits a number of notable features. First, for each Y', there is maximum in γ corresponding to an optimal wavelength. The curves do not approach infinity as the wavelength approaches zero; instead, the damping associated with the effective lattice viscosity, appearing as a k^{-3} dependence in Equation 2.6, supresses RT growth for very short wavelengths. Second, the disparity between RT growth rates for different yield strengths diminishes very strongly as the wavelength increases. That is, the RT instability, as modeled by Colvin *et al.*, is much more sensitive to the yield strength at shorter wavelengths, assuming the wavelength is not short enough for the effective lattice viscosity to damp the perturbation growth. Finally, we note that the thickness h of the plate plays a significant role, through the effective acceleration and the tanh term. This explains the much higher growth rates observed (1/ns scale) for the case of Lorenz *et al.*, compared to those observed for the aluminum/copper case (1/μs scale).

Based on the theory of Colvin *et al.*, then, a measurement technique for yield strength based on observed RT growth under known acceleration seems possible, and the theory suggests that such a technique would operate most effectively at short wavelengths, where both the predicted RT growth rate and the sensitivity of the growth rate to the yield strength are greatest. Such a measurement technique would benefit from the fact that it does not rely on shock loading and may therefore be used to characterize a material's yield strength in off-Hugoniot, quasi-isentropic states. Further, because the material deformation of interest may take place in the interior of the sample, a window is not needed to delay the arrival of the release wave at the interface. This removes the limitation on the driving pressure posed by the need to maintain the transparency of the window.

It is important to note here that a number of objections may be made to the theory of Colvin *et al.* Most significantly, Colvin's theory treats the medium as a fluid throughout the entire course of its acceleration and deformation, thus inherently ignoring any resistance to deformation associated with elastic effects in the medium. Further, it is an *ad hoc* analogy between stresses in a Newtonian fluid and stresses in a plastically deforming solid that yields the approximation shown above in Equation 2.2. Robinson and Swegle (1989) [6] also have shown that the temporal and spatial distribution of forces in deforming solids makes systems such as these very different from those considered in the theory of RT instability for fluids. Finally, the consideration of elastic stability is absent in the theory of Colvin *et al.*, and Terrones (2007) [7] demonstrates that deformation of solid bodies that are in fact elastically stable has often been attributed erroneously to RT instability.

3 PULSED-POWER EXPERIMENTS FOR MEASURING STRENGTH VIA RT INSTABILITY

Rayleigh-Taylor growth in solids has been exploited to measure strength in a number of experimental studies, beginning with the work of Miles (1966) [8] and Barnes (1974) [9]. Typically, these experimental studies have used expanding detonation products as the driver (or laser-ablated plasma stagnation in the case of Lorenz *et al.*). In order to achieve both a stronger and a more well-characterized drive history, as well as an increased pulse duration and smooth, isentropic loading, it is speculated that the strong magnetic fields and magnetic pressures developed in modern pulsed power devices could be used in such experiments. In particular, proof-of-principle experiments are planned for the Veloce device [10] at Sandia National Laboratories. This device is capable of current pulses up to 2.5 MA in amplitude and 2 μs in duration, which, it is estimated, can be used to deliver a pressure pulse of up to 10 GPa to a sample.

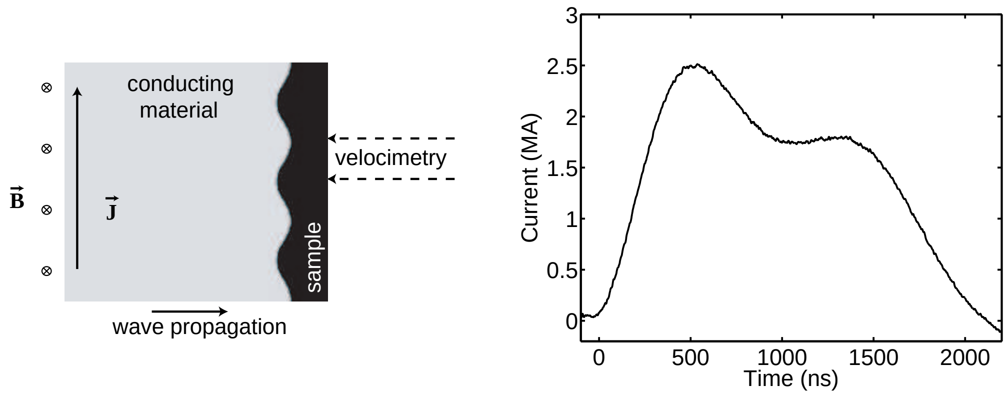

Fig. 3.2. Left: schematic setup in experiments planned for the Veloce device [10] to measure material strength using RT instability. $\vec{\mathbf{J}}$ denotes the current density vector and $\vec{\mathbf{B}}$ the magnetic flux density vector. Right: current pulse generated by Veloce.

The setup of such experiments is shown in Figure 3.2. The sample will consist of two layers of material: a thick layer of a well-characterized, conducting material, and a thinner layer of some sample material, separated by a planar interface with a machined perturbation. Current will flow initially in a sheet along the surface of the thicker layer, generating a region of strong magnetic field and magnetic pressure. This will initiate the propagation of a stress wave and a magnetic diffusion front from the free surface into the sample material. The stress wave will propagate across the sample and accelerate the interface, driving variable-acceleration RT instability due to the pressure gradient associated with the shape and propagation of the stress wave. The thicker conductor layer is necessary in the setup in order to delay the arrival of the magnetic diffusion front and the consequent onset of intense Ohmic heating. Optical velocimetry will be used to record the motion of the sample material free surface, from which RT growth rates may be computed. The current pulse driving this process is shown in Figure 3.2.

4 SIMULATIONS FOR MAGNETICALLY-DRIVEN RT INSTABILITY IN SOLIDS

Any of a variety of schemes may then be used to infer material strength or strength model parameter modifications from the RT growth data, by use of analytical methods or recursive numerical simulations. In the case of elastic deformation and constant acceleration, analytical techniques may be useful, but at pressures on the order of 10^{10} Pa or higher, and in the transient environment of pulsed power devices, simulation-based schemes will be most effective. Assuming the Steinberg-Guinan (SG) strength model (Equation 2) accurately captures the form of the functional dependence of the yield strength on the state of the material, the model parameters may be manipulated artificially, following the approach of Lorenz *et al.*, to find by recursive simulations the effective strength enhancement that allows the simulations to reproduce the observed behavior. This can be done for the high-pressure, high-deformation experiments considered here by modifying three tabulated parameters in the SG model: (1) the pressure-hardening coefficient A, (2) the strain-hardening coefficient B, and (3) the strain-hardening exponent n.

Simulations are performed using the finite-element multimaterial MHD code ALEGRA [11]. ALEGRA has been used extensively and successfully in simulations of this type for magnetically accelerated solid materials [12]. Recent tests have demonstrated the ability to reproduce the expected deformation and yield behavior in 1D, single-material, stress-wave tests in aluminum and tungsten, and recover nearly the same RT growth data reported by Lorenz *et al.* in 2D simulations for their plasma-piston-driven experiments, to within the experimental error ranges. The present Eulerian simulations are set up on a 2D, uniform Cartesian mesh, using the Lagrange-remap method implemented in ALEGRA. The initial condition is shown schematically in Figure XX, where the stress and magnetic diffusion waves propagate in the $+x$-direction, and the interfacial perturbation is imposed along the y-direction. Periodic boundary conditions are imposed at the y-boundaries, with the domain y-dimension set equal to the perturbation wavelength λ, and the current history shown in Figure 3.2 is coupled to the simulation through a boundary condition imposed at the -x-boundary, which allows current to flow in the y-direction on the boundary. The associated magnetic field develops a magnetic pressure, which drives a smooth (nearly isentropic) stress wave, followed by a magnetic diffusion wave, into the conducting material. The gradient in stress associated with this wave provides a variable (but not impulsive) acceleration to the interface, whose subsequent deformation exhibits many of the typical features of RT instability. It is important to note that the acceleration is provided almost entirely by the stress gradient, not by the $\mathbf{J} \times \mathbf{B}$ force, since the magnetic diffusion wave is significantly delayed relative to the stress wave.

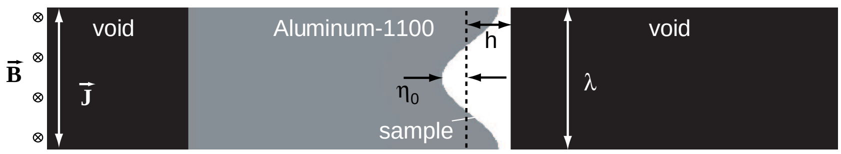

Fig. 4.3. Setup for ALEGRA simulations, showing current density **J** imposed by boundary conditions; perturbation wavelength λ and initial amplitude η_0; and sample thickness h.

A series of simulations are performed using various sample materials: vanadium, copper, tungsten, gold, and lead. Further, variable sample thicknesses h, perturbation wavelengths λ, and initial amplitudes η_0 are also used. The conducting material used to resist the magnetic diffusion wave propagation is aluminum-1100, with a thickness of 0.1 cm. In these simulations, tabular (Sesame) equations of state are used for the two solid materials, with Lee-More-Desjarlais electrical conductivity models, and Steinberg-Guinan strength models.

REFERENCES

[1] Colvin, J.D., Legrand, M., Remington, B.A., Schurtz, G and Weber, S.V. 2003. A model for instability growth in accelerated solid metals, *J. Appl. Phys.*, **93**(9), pp. 5287–5301.

[2] Steinberg, D.J., Cochran, S.G., and Guinan, M.W. 2004. A constitutive model for metals applicable at high-strain rate, *J. Appl. Phys.*, **51**(3), pp. 1498–1504.

[3] Mikaelian, K.O. 2004. Rayleigh-Taylor instability in finite-thickness fluids with viscosity and surface tension, *Phys. Rev. E*, **54**(4), pp. 3676–3680.

[4] Chandrasekhar, S. 1968. *Hydrodyamic and Hydromagnetic Stability*, Oxford University Press, London.

[5] Lorenz, K.T., Edwards, M.J., Glendinning, S.G., Jankowski, A.F., McNaney. J., Pollaine, S.M., and Remington, B.A. 2005. Assessing ultrahigh-pressure, quasi-isentropic states of matter, *Phys. Plasmas*, **12**, 056309.

[6] Robinson, A.C. and Swegle, J.W. 1989. Acceleration instability in elastic-plastic solids. II. Analytical techniques, *J. Appl. Phys.*, **66**(7), pp. 2859–2872.

[7] Terrones, G. 2007. Elastic instability and the onset of plastic flow in accelerated solid plates, *J. Appl. Phys.*, **102**, 034908.

[8] Miles, J.W. 1966. Taylor instability of a flat plate, General Dynamics Report No. GAMD-7335, AD643161 (unpublished).

[9] Barnes, J.F., Blewett, P.J., McQueen, R.G., Meyer, K.A., and Venable, D. 1974. Taylor instability in solids, *J. Appl. Phys.*, **45**(2), pp. 727–732.

[10] Ao, T., Asay, J.R., Chantrenne, S., Baer, M.R., and Hall, C.A. 2008. A compact strip-line pulsed power generator for isentropic compression experiments, *Rev. Sci. Instrum.*, **79**, 013903.

[11] Robinson, A.C., Rider, W.J., et al. 2008 ALEGRA: An arbitrary Lagrangian-Eulerian multimaterial, multiphysics code. In *Proceedings of the 46th AIAA Aerospace Sciences Meeting, Reno, NV, January 2008.*

[12] Lemke, R.W., Knudson, M.D., Robinson, A.C., Haill, T.A., Struve, K.W., Asay, J.R., and Mehlhorn, T.A. 2003. Self-consistent, two-dimensional, magnetohydrodynamic simulations of magnetically driven flyer plates, *Phys. Plasmas*, **10**(5), pp. 1867–1874.